A Hybrid Second Moment Method for Thermal Radiative Transfer

M&C 2025

M. Pozulp[1,3], T. Haut[1], P. Brantley[1], S. Olivier[2], J. Vujic[3]

[1]Lawrence Livermore National Laboratory
[2]Los Alamos National Laboratory
[3]University of California, Berkeley

April 29, 2025

LLNL-PRES-2005149

This work was performed under the auspices of the U.S. Department of Energy by Lawrence Livermore National Laboratory under contract DE-AC52-07NA27344. Lawrence Livermore National Security, LLC

We describe a new method that did not immediately work.

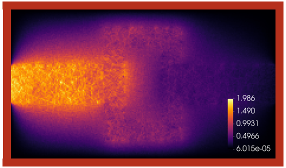

Hybrid Second Moment Method

Numerical Results

Noisy Crooked Pipe

We needed variance reduction.

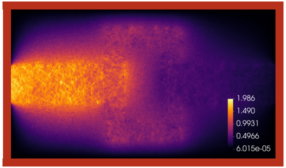

Hybrid Second Moment Method

Numerical Results

- **Noisy Crooked Pipe**

Variance Reduction

Fixing the noise issue created a new problem.

Hybrid Second Moment Method

Numerical Results

Noisy Crooked Pipe

Variance Reduction

Incorrect Crooked Pipe

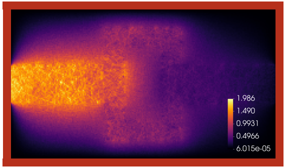

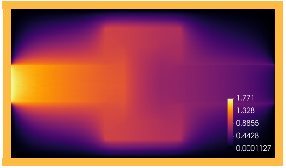

We fixed that problem too.

Hybrid Second Moment Method

Numerical Results

- **Noisy Crooked Pipe**

Variance Reduction

- **Incorrect Crooked Pipe**
- **Correct Crooked Pipe**

Conclusion

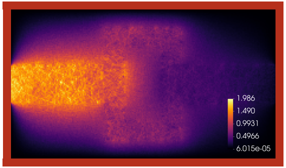

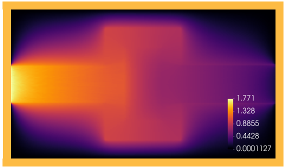

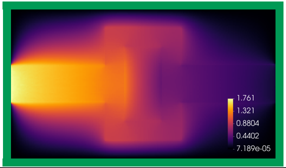

Hybrid Second Moment (HSM) solves a linear transport equation.

$$\mathbf{\Omega} \cdot \nabla \psi + \sigma_t \psi = \frac{\sigma_s}{4\pi} \int_{\mathbb{S}^2} \psi \, \mathrm{d}\Omega' + q$$

Subject to an inflow boundary condition.

$$\mathbf{\Omega} \cdot \nabla \psi + \sigma_t \psi = \frac{\sigma_s}{4\pi} \int_{\mathbb{S}^2} \psi \, \mathrm{d}\Omega' + q \,, \tag{1a}$$

$$\psi(\mathbf{x}, \mathbf{\Omega}) = \psi_{\mathsf{inc}}(\mathbf{x}, \mathbf{\Omega}) \,, \quad \mathbf{x} \in \partial\mathcal{D} \text{ and } \mathbf{\Omega} \cdot \mathbf{n} < 0 \,. \tag{1b}$$

This system is an equivalent reformulation of eqs. (1a) and (1b).

$$\nabla \cdot \boldsymbol{J} + \sigma_a \varphi = Q_0, \quad \mathbf{x} \in \mathcal{D}\,, \tag{2a}$$

$$\frac{1}{3}\nabla \varphi + \sigma_t \boldsymbol{J} = \boldsymbol{Q}_1 - \nabla \cdot \mathbf{T}, \quad \mathbf{x} \in \mathcal{D}\,. \tag{2b}$$

$$\boldsymbol{J} \cdot \mathbf{n} = \frac{1}{2}\varphi + 2J_{\mathsf{in}} + \beta, \quad \mathbf{x} \in \partial\mathcal{D}\,. \tag{2c}$$

We compute the scattering using φ from the moment system.

$$\boldsymbol{\Omega} \cdot \nabla \psi + \sigma_t \psi = \frac{\sigma_s}{4\pi} \varphi + q \,,$$

$$\psi(\mathbf{x}, \boldsymbol{\Omega}) = \bar{\psi}(\mathbf{x}, \boldsymbol{\Omega}) \,, \quad \mathbf{x} \in \partial\mathcal{D} \text{ and } \boldsymbol{\Omega} \cdot \mathbf{n} < 0 \,.$$

We estimate T and β using Monte Carlo.

$$\mathbf{\Omega} \cdot \nabla \psi + \sigma_t \psi = \frac{\sigma_s}{4\pi} \varphi + q \,,$$

$$\psi(\mathbf{x}, \mathbf{\Omega}) = \bar{\psi}(\mathbf{x}, \mathbf{\Omega}) \,, \quad \mathbf{x} \in \partial \mathcal{D} \text{ and } \mathbf{\Omega} \cdot \mathbf{n} < 0 \,.$$

$$\mathbf{T}(\psi) = \int_{\mathbb{S}^2} \mathbf{\Omega} \otimes \mathbf{\Omega} \, \psi \, \mathrm{d}\Omega - \tfrac{1}{3} \mathbf{I} \int_{\mathbb{S}^2} \psi \, \mathrm{d}\Omega$$

$$\beta(\psi) = \int_{\mathbb{S}^2} |\mathbf{\Omega} \cdot \mathbf{n}| \, \psi \, \mathrm{d}\Omega - \tfrac{1}{2} \int_{\mathbb{S}^2} \psi \, \mathrm{d}\Omega$$

We solve the moment system using the finite element method.

$$\boldsymbol{\Omega}\cdot\nabla\psi + \sigma_t\psi = \frac{\sigma_s}{4\pi}\varphi + q\,,$$
$$\psi(\mathbf{x},\boldsymbol{\Omega}) = \bar{\psi}(\mathbf{x},\boldsymbol{\Omega})\,, \quad \mathbf{x}\in\partial\mathcal{D} \text{ and } \boldsymbol{\Omega}\cdot\mathbf{n} < 0\,.$$

$$\nabla\cdot\boldsymbol{J} + \sigma_a\varphi = Q_0\,, \quad \mathbf{x}\in\mathcal{D}\,,$$
$$\tfrac{1}{3}\nabla\varphi + \sigma_t\boldsymbol{J} = \boldsymbol{Q}_1 - \nabla\cdot\mathbf{T}\,, \quad \mathbf{x}\in\mathcal{D}\,,$$
$$\boldsymbol{J}\cdot\mathbf{n} = \tfrac{1}{2}\varphi + 2J_{\text{in}} + \beta\,, \quad \mathbf{x}\in\partial\mathcal{D}\,.$$

$$\mathbf{T}(\psi) = \int_{\mathbb{S}^2}\boldsymbol{\Omega}\otimes\boldsymbol{\Omega}\,\psi\,\mathrm{d}\Omega - \tfrac{1}{3}\mathbf{I}\int_{\mathbb{S}^2}\psi\,\mathrm{d}\Omega$$
$$\beta(\psi) = \int_{\mathbb{S}^2}|\boldsymbol{\Omega}\cdot\mathbf{n}|\,\psi\,\mathrm{d}\Omega - \tfrac{1}{2}\int_{\mathbb{S}^2}\psi\,\mathrm{d}\Omega$$

We iterate to converge the scattering source.

$$\begin{aligned} \boldsymbol{\Omega} \cdot \nabla \psi + \sigma_t \psi &= \frac{\sigma_s}{4\pi} \varphi + q \,, \\ \psi(\mathbf{x}, \boldsymbol{\Omega}) &= \bar{\psi}(\mathbf{x}, \boldsymbol{\Omega}) \,, \quad \mathbf{x} \in \partial\mathcal{D} \text{ and } \boldsymbol{\Omega} \cdot \mathbf{n} < 0 \,. \end{aligned}$$

$$\varphi$$

$$\begin{aligned} \nabla \cdot \boldsymbol{J} + \sigma_a \varphi &= Q_0 \,, \quad \mathbf{x} \in \mathcal{D} \,, \\ \tfrac{1}{3} \nabla \varphi + \sigma_t \boldsymbol{J} &= \boldsymbol{Q}_1 - \nabla \cdot \mathbf{T} \,, \quad \mathbf{x} \in \mathcal{D} \,, \\ \boldsymbol{J} \cdot \mathbf{n} &= \tfrac{1}{2} \varphi + 2 J_{\text{in}} + \beta \,, \quad \mathbf{x} \in \partial\mathcal{D} \,. \end{aligned}$$

$$\mathbf{T}(\psi) = \int_{\mathbb{S}^2} \boldsymbol{\Omega} \otimes \boldsymbol{\Omega} \, \psi \, \mathrm{d}\Omega - \tfrac{1}{3} \mathbf{I} \int_{\mathbb{S}^2} \psi \, \mathrm{d}\Omega$$

$$\beta(\psi) = \int_{\mathbb{S}^2} |\boldsymbol{\Omega} \cdot \mathbf{n}| \, \psi \, \mathrm{d}\Omega - \tfrac{1}{2} \int_{\mathbb{S}^2} \psi \, \mathrm{d}\Omega$$

The Crooked Pipe is commonly used for comparing methods.

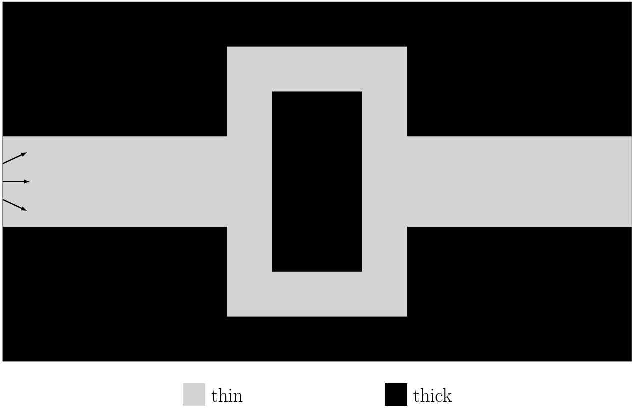

We use a mesh of squares of equal size.

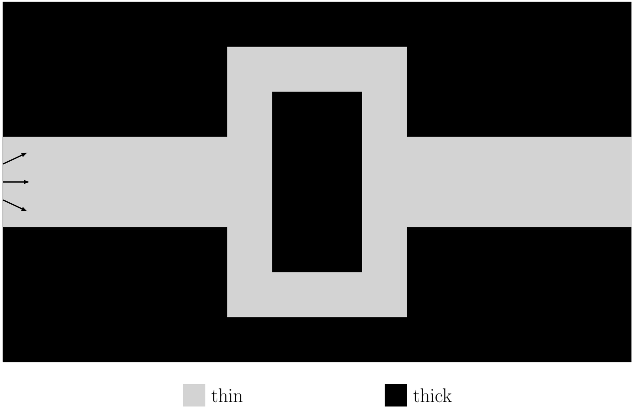

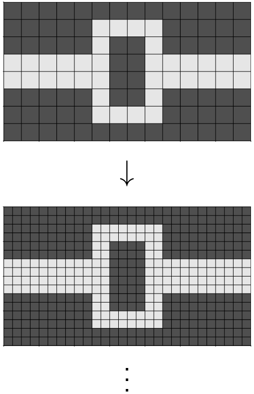

$$224 \times 128 = 28,672$$

The horizontal symmetry of CP allows top/bottom plots.

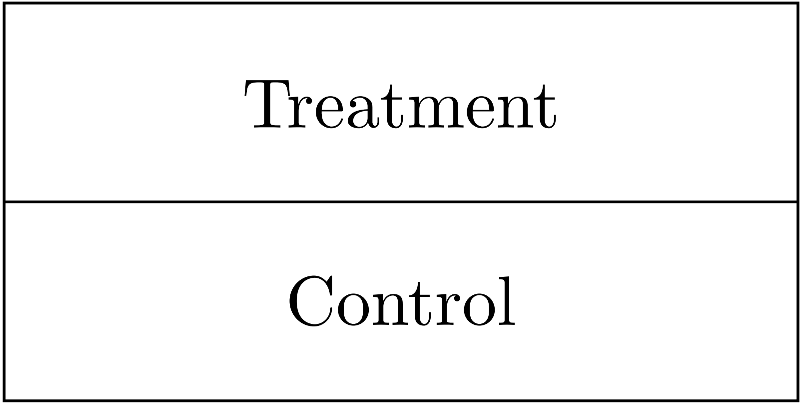

Our method is much more noisy than unaccelerated Monte Carlo.

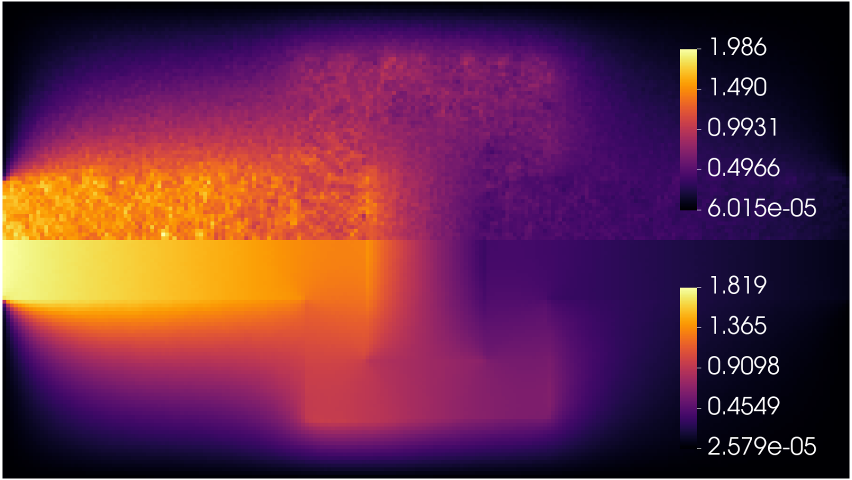

The rest of this talk is about variance reduction.

~~Hybrid Second Moment Method~~

~~Numerical Results~~

- ~~**Noisy Crooked Pipe**~~

Variance Reduction

- **Incorrect Crooked Pipe**
- **Correct Crooked Pipe**

Conclusion

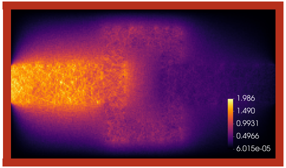

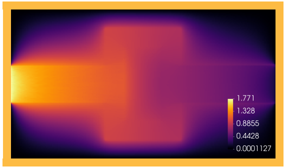

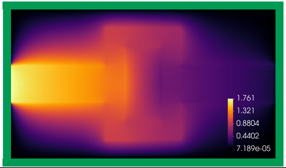

The thick diffusion limit is when $\epsilon \in (0, 1] \to 0$.

$$\sigma_t = 1/\epsilon \,, \tag{3a}$$

$$\sigma_a = \epsilon \,, \tag{3b}$$

$$\sigma_s = \sigma_t - \sigma_a \,, \tag{3c}$$

$$q = \epsilon \,. \tag{3d}$$

The variance depends on the magnitude of the source function.

Theorem

Let $Q = \frac{\sigma_s}{4\pi}\varphi + q$ *such that,*

$$\mathbf{\Omega} \cdot \nabla\psi + \sigma_t\psi = Q\,.$$

Then $\mathrm{Var}[\cdot]$ *is,*

$$\left(\mathrm{order}(Q)\right)^2 \epsilon\,.$$

Compute the deviation of the intensity from isotropy.

Substitute $\psi = \frac{\varphi}{4\pi} + \tilde{\psi}$ into:

$$\mathbf{\Omega} \cdot \nabla \psi + \sigma_t \psi = \frac{\sigma_s}{4\pi} \varphi + q \,,$$

to get,

$$\mathbf{\Omega} \cdot \nabla \tilde{\psi} + \sigma_t \tilde{\psi} = -\frac{1}{4\pi} \left(\sigma_a \varphi + \mathbf{\Omega} \cdot \nabla \varphi \right) + q \,. \tag{4}$$

The new solution is incorrect on material interfaces.

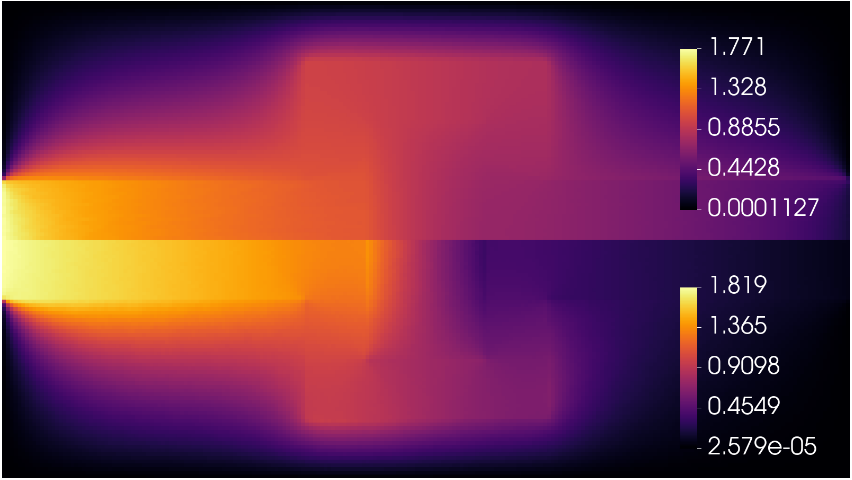

Modify the approach by replacing φ with $\bar{\varphi}$.

Before, we substituted $\psi = \frac{\varphi}{4\pi} + \tilde{\psi}$ to get:

$$\boldsymbol{\Omega} \cdot \nabla \tilde{\psi} + \sigma_t \tilde{\psi} = -\frac{1}{4\pi}(\sigma_a \varphi + \boldsymbol{\Omega} \cdot \nabla \varphi) + q \,.$$

Now, substitute $\psi = \frac{\bar{\varphi}}{4\pi} + \tilde{\psi}$ to get:

$$\boldsymbol{\Omega} \cdot \nabla \tilde{\psi} + \sigma_t \tilde{\psi} = \frac{\sigma_t}{4\pi}(\varphi - \bar{\varphi}) - \frac{1}{4\pi}(\sigma_a \varphi + \boldsymbol{\Omega} \cdot \nabla \bar{\varphi}) + q \,. \tag{5}$$

How should we choose $\bar{\varphi}$?

Requirements:

1. $\nabla \bar{\varphi}$ is well-defined

2. $\varphi - \bar{\varphi}$ is $O(1/\sigma_t)$

Solve a transient heat conduction equation for $\bar{\varphi}$.

Requirements:

1. $\nabla \bar{\varphi}$ is well-defined
2. $\varphi - \bar{\varphi}$ is $O(1/\sigma_t)$

$$\frac{\partial \bar{\varphi}}{\partial t} = \nabla \cdot \frac{1}{\sigma_t} \nabla \bar{\varphi}, \quad \mathbf{x} \in \mathcal{D}\,, \tag{6}$$

Take one timestep,

$$\frac{\Delta t}{h^2} \frac{1}{\max_{\mathbf{x}} \sigma_t} \ll 1\,. \tag{7}$$

The solution on material interfaces is no longer incorrect.

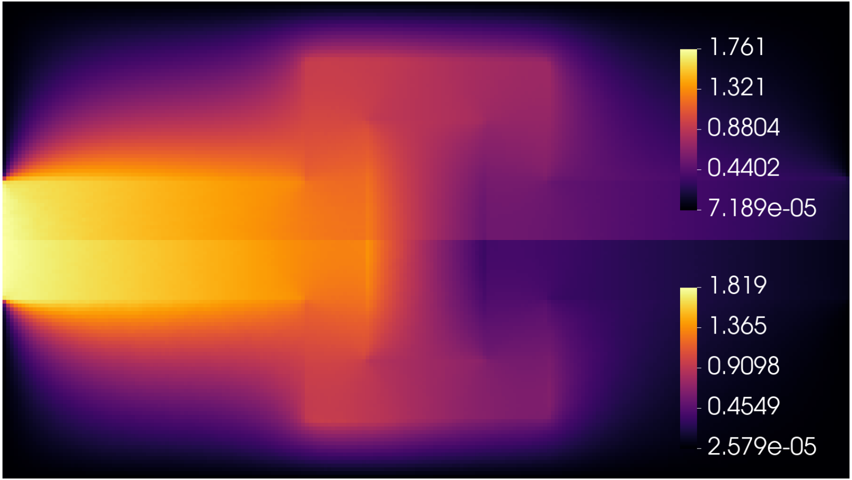

The noise is gone, and the solution is not incorrect.

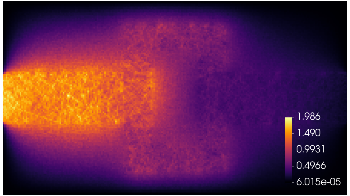

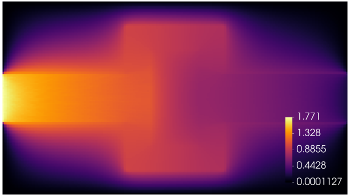

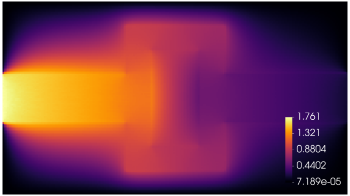

Our method runs very fast.

	Runtime
HSM	0m 22s
UMC	41m 35s

The figure of merit is much higher for HSM than for UMC.

	Runtime	Variance	FOM
HSM	0m 22s	$3.66 \cdot 10^{-4}$	124.2
UMC	41m 35s	$5.20 \cdot 10^{-5}$	7.7

We conclude that our hybrid method seems useful.

~~Hybrid Second Moment Method~~

~~Numerical Results~~

- ~~Noisy Crooked Pipe~~

~~Variance Reduction~~

- ~~Incorrect Crooked Pipe~~
- ~~Correct Crooked Pipe~~

~~Conclusion~~

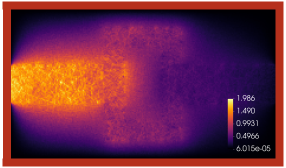

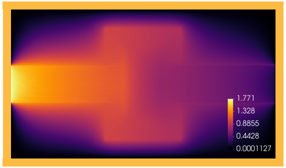

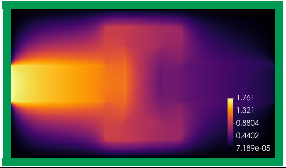

Could it be competitive with DDMC?

	HSM	DDMC
Orders of magnitude speedups	✓	✓
No diffusion approximation	✓	×
No phase-space partitioning	✓	×
No issues with unstructured meshes	✓	×
No iteration	×	✓
No linear solver	×	✓
No negative energy-weight	×	✓
Demonstrated in production calculations	×	✓

Extra slides.

We describe a new hybrid method that did not immediately work.

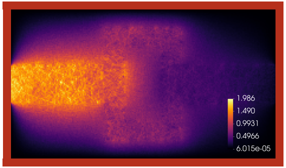

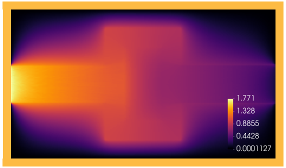

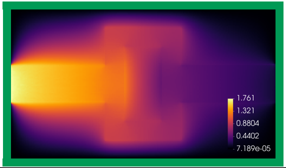

Can we make Monte Carlo faster without sacrificing accuracy?

- Why Monte Carlo?
- Why IMC?
- Why not RW?
- Why not DDMC?
- Why not Cooper, Lam, Novellino, Park, Pasmann, Willert, or any other hybrid methods?

Progress Porting LLNL Monte Carlo Transport Codes to the AMD Instict MI300A APU at 1:25 PM today in Special Session on GPU Computing

llnl.gov/article/52336/llnl-dedicates-el-capitan-ushering-new-era-supercomputing-national-security

Hybrid Second Moment (HSM) solves a linear transport equation.

$$\boldsymbol{\Omega} \cdot \nabla \psi + \sigma_t \psi = \frac{\sigma_s}{4\pi} \int_{\mathbb{S}^2} \psi \, \mathrm{d}\Omega' + q \,, \tag{8a}$$

$$\psi(\mathbf{x}, \boldsymbol{\Omega}) = \psi_{\mathsf{inc}}(\mathbf{x}, \boldsymbol{\Omega}) \,, \quad \mathbf{x} \in \partial\mathcal{D} \text{ and } \boldsymbol{\Omega} \cdot \mathbf{n} < 0 \,. \tag{8b}$$

This system is an equivalent reformulation of eqs. (8a) and (8b).

$$\nabla \cdot \boldsymbol{J} + \sigma_a \varphi = Q_0, \quad \mathbf{x} \in \mathcal{D}\,, \tag{9a}$$

$$\frac{1}{3}\nabla \varphi + \sigma_t \boldsymbol{J} = \boldsymbol{Q}_1 - \nabla \cdot \mathbf{T}, \quad \mathbf{x} \in \mathcal{D}\,. \tag{9b}$$

$$\boldsymbol{J} \cdot \mathbf{n} = \frac{1}{2}\varphi + 2J_{\mathsf{in}} + \beta, \quad \mathbf{x} \in \partial\mathcal{D}\,. \tag{9c}$$

The Second Moment Method iterates the scattering source.

$$\varphi$$

$$\begin{aligned}\boldsymbol{\Omega}\cdot\nabla\psi + \sigma_t\psi &= \frac{\sigma_s}{4\pi}\varphi + q\,, \\ \psi(\mathbf{x},\boldsymbol{\Omega}) &= \bar{\psi}(\mathbf{x},\boldsymbol{\Omega})\,, \quad \mathbf{x}\in\partial\mathcal{D} \text{ and } \boldsymbol{\Omega}\cdot\mathbf{n} < 0\,.\end{aligned}$$

$$\begin{aligned}\nabla\cdot\boldsymbol{J} + \sigma_a\varphi &= Q_0\,, \quad \mathbf{x}\in\mathcal{D}\,, \\ \tfrac{1}{3}\nabla\varphi + \sigma_t\boldsymbol{J} &= \boldsymbol{Q}_1 - \nabla\cdot\mathbf{T}\,, \quad \mathbf{x}\in\mathcal{D}\,, \\ \boldsymbol{J}\cdot\mathbf{n} &= \tfrac{1}{2}\varphi + 2J_{\text{in}} + \beta\,, \quad \mathbf{x}\in\partial\mathcal{D}\,.\end{aligned}$$

$$\mathbf{T}(\psi) = \int_{\mathbb{S}^2}\boldsymbol{\Omega}\otimes\boldsymbol{\Omega}\,\psi\,\mathrm{d}\Omega - \tfrac{1}{3}\mathbf{I}\int_{\mathbb{S}^2}\psi\,\mathrm{d}\Omega$$

$$\beta(\psi) = \int_{\mathbb{S}^2}|\boldsymbol{\Omega}\cdot\mathbf{n}|\,\psi\,\mathrm{d}\Omega - \tfrac{1}{2}\int_{\mathbb{S}^2}\psi\,\mathrm{d}\Omega$$

The deterministic component of HSM solves the moment system.

Find $(\varphi, \boldsymbol{J}) \in Y_p \times RT_p$ such that,

$$\int u \, \nabla \cdot \boldsymbol{J} \, \mathrm{d}\mathbf{x} + \int \sigma_a \, u\varphi \, \mathrm{d}\mathbf{x} = \int u \, Q_0 \, \mathrm{d}\mathbf{x} \, , \quad \forall u \in Y_p \, , \tag{10a}$$

$$-\frac{1}{3} \int \nabla \cdot \boldsymbol{v} \, \varphi \, \mathrm{d}\mathbf{x} + \int \sigma_t \, \boldsymbol{v} \cdot \boldsymbol{J} \, \mathrm{d}\mathbf{x} + \frac{2}{3} \int_{\Gamma_b} (\boldsymbol{v} \cdot \mathbf{n})(\boldsymbol{J} \cdot \mathbf{n}) \, \mathrm{d}s = \int \boldsymbol{v} \cdot \boldsymbol{Q}_1 \, \mathrm{d}\mathbf{x} - \int_{\Gamma_b} \boldsymbol{v} \cdot \mathbf{T}\mathbf{n} \, \mathrm{d}s$$
$$+ \frac{2}{3} \int_{\Gamma_b} (\boldsymbol{v} \cdot \mathbf{n})(2 J_{\mathsf{in}} + \beta) \, \mathrm{d}s - \int_{\Gamma_0} [\![v]\!] \cdot \{\!\{ \mathbf{T}\mathbf{n} \}\!\} \, \mathrm{d}s + \int \nabla_h \boldsymbol{v} : \mathbf{T} \, \mathrm{d}\mathbf{x} \quad \forall \boldsymbol{v} \in RT_p \, . \tag{10b}$$

The Monte Carlo component of HSM has no scattering events.

Estimate $\hat{\mathbf{T}} = \hat{\mathbf{P}} - \frac{1}{3}\mathbf{I}\hat{\phi}$ and $\hat{\beta} = \hat{B} - \frac{1}{2}\hat{\phi}_s$ using:

$$\hat{\phi} = \frac{1}{V}\sum_i d_i w_i \,, \qquad \hat{\mathbf{P}} = \frac{1}{V}\sum_i \boldsymbol{\Omega}_i \otimes \boldsymbol{\Omega}_i \, d_i w_i \,, \tag{11a}$$

$$\hat{B} = \frac{2}{A}\sum_i w_i \,, \qquad \hat{\phi}_s = \frac{2}{A}\sum_i \frac{w_i}{|\boldsymbol{\Omega}_i \cdot \mathbf{n}|} \,. \tag{11b}$$

While solving:

$$\boldsymbol{\Omega} \cdot \nabla\psi + \sigma_t \psi = \frac{\sigma_s}{4\pi}\varphi + q \,, \tag{12a}$$

$$\psi(\mathbf{x}, \boldsymbol{\Omega}) = \psi_{\mathsf{inc}}(\mathbf{x}, \boldsymbol{\Omega}) \,, \quad \mathbf{x} \in \partial\mathcal{D} \text{ and } \boldsymbol{\Omega} \cdot \mathbf{n} < 0 \,. \tag{12b}$$

Using MC allows us to move fixed sources out of the iteration.

$\hat{\phi}^{(0)}, \hat{\mathbf{T}}^{(0)}, \hat{\beta}^{(0)} \leftarrow \mathsf{mc}(q,\ \psi_{\mathsf{inc}})$ ▷ Sample the fixed sources q and ψ_{inc}

$i \leftarrow 1$

while not converged$(\hat{\phi}^{(i-1)}, \hat{\phi}^{(i)})$ **do**

  $\varphi^{(i)} \leftarrow \mathsf{sm}(Q_0, \boldsymbol{Q}_1, \hat{\mathbf{T}}^{(i-1)}, \hat{\beta}^{(i-1)})$

  $\hat{\phi}_{\mathsf{temp}}, \hat{\mathbf{T}}_{\mathsf{temp}}, \hat{\beta}_{\mathsf{temp}} \leftarrow \mathsf{mc}(\varphi^{(i)})$ ▷ Sample the variable source $\frac{\sigma_s}{4\pi}\varphi^{(i)}$

  $\hat{\phi}^{(i)} \leftarrow \hat{\phi}^{(0)} + \hat{\phi}_{\mathsf{temp}}$

  $\hat{\mathbf{T}}^{(i)} \leftarrow \hat{\mathbf{T}}^{(0)} + \hat{\mathbf{T}}_{\mathsf{temp}}$

  $\hat{\beta}^{(i)} \leftarrow \hat{\beta}^{(0)} + \hat{\beta}_{\mathsf{temp}}$

  $i \leftarrow i + 1$

end while

return $\hat{\phi}^{(i)}$

The HSM error surface height is lowest in the north-east.

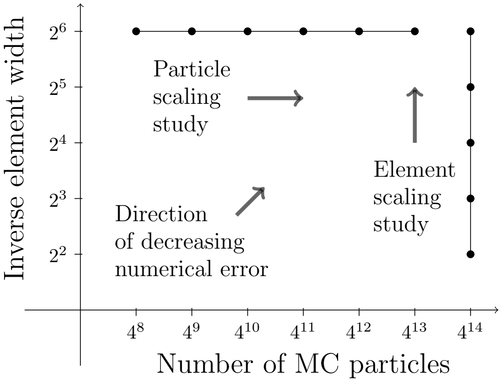

The HSM error is:

$$O(h) + O(N^{-1/2})$$

We verified HSM using the Method of Manufactured Solutions.

$$\psi_{\mathsf{MMS}}(\mathbf{x}, \mathbf{\Omega}) = \frac{1}{4\pi}\Big(\sin(\pi x)\sin(\pi y) + \mathbf{\Omega}_x\mathbf{\Omega}_y \sin(2\pi x)\sin(2\pi y)$$
$$+ \mathbf{\Omega}_x^2 \sin\left(\frac{5\pi}{2}x + \frac{\pi}{4}\right)\sin\left(\frac{5\pi}{2}y + \frac{\pi}{4}\right) + 0.5\Big)\,, \quad \text{(13a)}$$

$$\phi_{\mathsf{MMS}}(\mathbf{x}) = \int_{\mathbb{S}^2} \psi_{\mathsf{MMS}}(\mathbf{x}, \mathbf{\Omega})\,\mathrm{d}\Omega\,, \quad \text{(13b)}$$

$$\bar{\phi}_{\mathsf{MMS}}(x_1, x_2, y_1, y_2) = \frac{1}{((x_2 - x_1)(y_2 - y_1))}\int_{x_1}^{x_2}\int_{y_1}^{y_2} \phi_{\mathsf{MMS}}(\mathbf{x})\,\mathrm{d}y\,\mathrm{d}x\,. \quad \text{(13c)}$$

The MMS solution that we seek with HSM is a histogram.

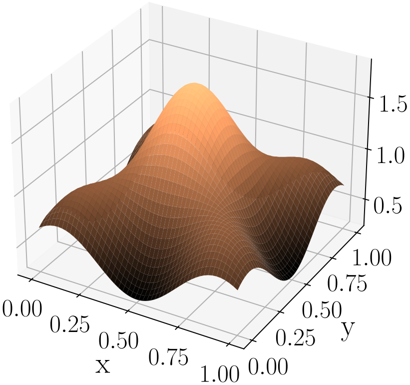

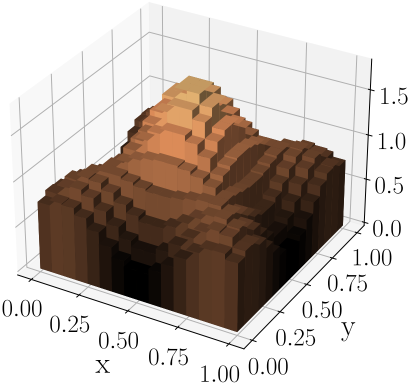

We observed the hypothesized error for the MMS problem.

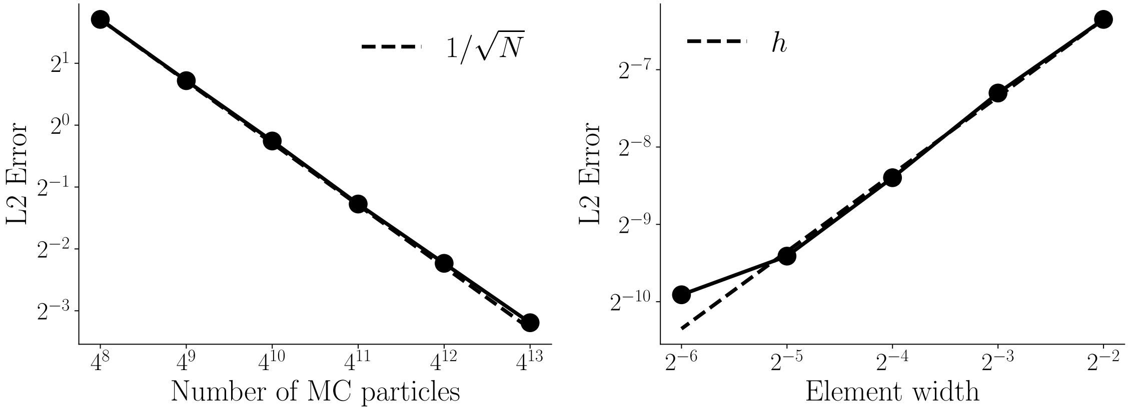

HSM is faster than unaccelerated MC (UMC) in the TDL.

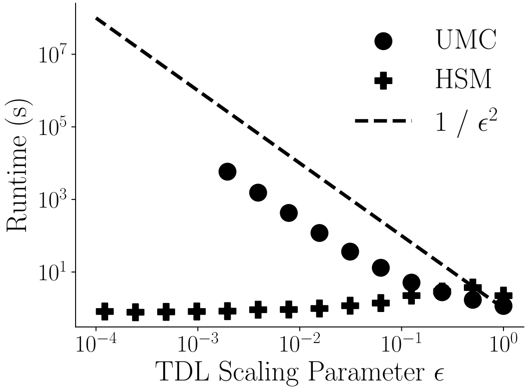

Thick Diffusion Limit (TDL):

$$\sigma_t \to \sigma_t/\epsilon \,, \tag{14a}$$

$$\sigma_a \to \epsilon\sigma_a \,, \tag{14b}$$

$$\sigma_s = \sigma_t - \sigma_a \,, \tag{14c}$$

$$q \to \epsilon q \,, \tag{14d}$$

for the TDL parameter $\epsilon \in (0, 1]$, and let:

$$\epsilon \to 0 \,. \tag{14e}$$

The Crooked Pipe is commonly used for comparing TRT methods.

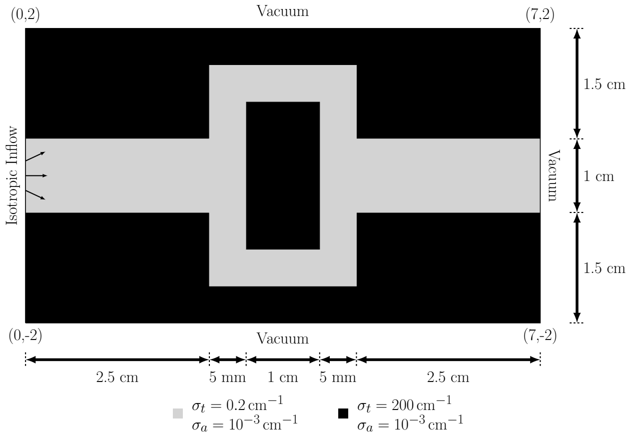

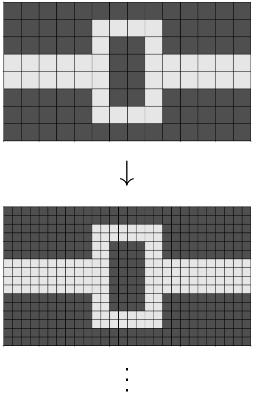

$$224 \times 128 = 28,672$$

The horizontal symmetry of CP allows top/bottom plots.

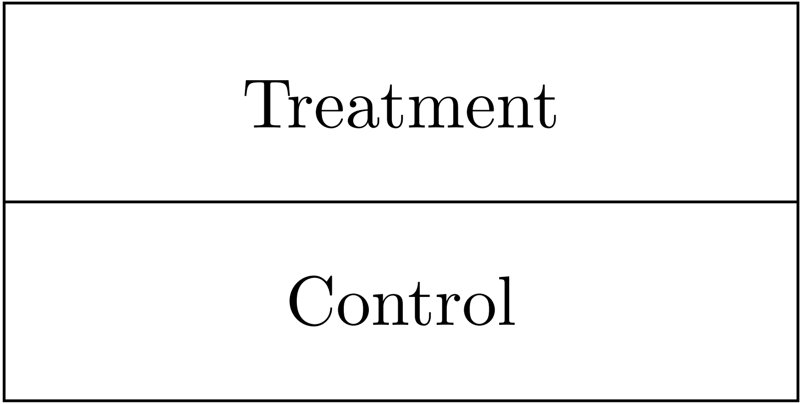

HSM is much more noisy than unaccelerated Monte Carlo.

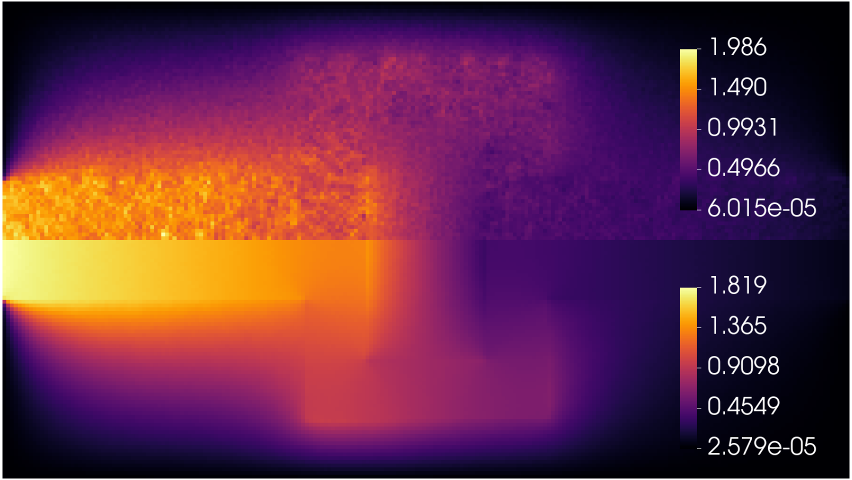

The HSM variance is very large in the Thick Diffusion Limit.

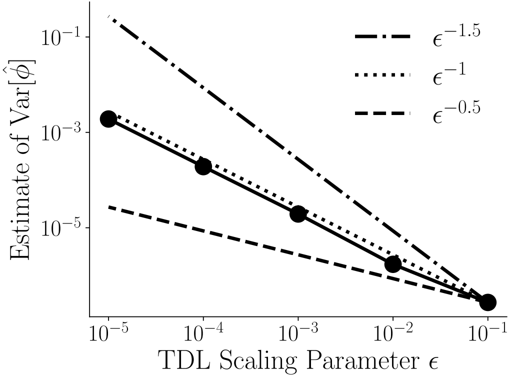

$$\mathrm{Var}[\hat{\phi}] \approx \frac{1}{600} \sum_{i=1}^{600} (\hat{\phi}_i - \Phi)^2 \, , \tag{15}$$

where Φ is the mean estimate defined by,

$$\Phi = \frac{1}{600} \sum_{i=1}^{600} \hat{\phi}_i \, . \tag{16}$$

The rest of this talk is about variance reduction.

- ~~Motivation~~
- ~~Prior Work~~
- ~~Hybrid Second Moment Method~~
  - ~~Deterministic Component of HSM~~
  - ~~Monte Carlo Component of HSM~~
- ~~Numerical Results~~
  - ~~Method of Manufactured Solutions Verification~~
  - ~~Noisy Crooked Pipe~~
- Variance Reduction
  - Difference Formulation
  - **Incorrect Crooked Pipe**
  - Generalized Difference Formulation
  - **Correct Crooked Pipe**
- Conclusion

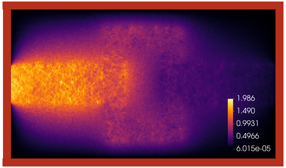

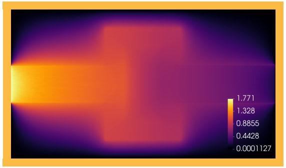

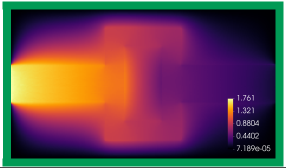

Compute the deviation of the intensity from isotropy.

Substitute $\psi = \frac{\varphi}{4\pi} + \tilde{\psi}$ into:

$$\boldsymbol{\Omega} \cdot \nabla \psi + \sigma_t \psi = \frac{\sigma_s}{4\pi} \varphi + q \,, \tag{17a}$$

$$\psi(\mathbf{x}, \boldsymbol{\Omega}) = \psi_{\mathsf{inc}}(\mathbf{x}, \boldsymbol{\Omega}) \,, \quad \mathbf{x} \in \partial \mathcal{D} \text{ and } \boldsymbol{\Omega} \cdot \mathbf{n} < 0 \,. \tag{17b}$$

to get,

$$\boldsymbol{\Omega} \cdot \nabla \tilde{\psi} + \sigma_t \tilde{\psi} = -\frac{1}{4\pi} (\sigma_a \varphi + \boldsymbol{\Omega} \cdot \nabla \varphi) + q \,, \tag{18a}$$

$$\tilde{\psi}(\mathbf{x}, \boldsymbol{\Omega}) = \psi_{\mathsf{inc}}(\mathbf{x}, \boldsymbol{\Omega}) - \frac{\varphi(\mathbf{x})}{4\pi} \,, \quad \mathbf{x} \in \partial \mathcal{D} \text{ and } \boldsymbol{\Omega} \cdot \mathbf{n} < 0 \,. \tag{18b}$$

This approach requires $\nabla\varphi$ and a variable boundary source.

	Fixed	Variable		
Volume	q	$\dfrac{\sigma_s}{4\pi}\varphi$	$O(\epsilon)$	$O(1/\epsilon)$
Boundary	ψ_{inc}	0	$O(1)$	N/A
Volume	q	$-\frac{1}{4\pi}(\sigma_a\varphi + \mathbf{\Omega}\cdot\nabla\varphi)$	$O(\epsilon)$	$O(1)$
Boundary	ψ_{inc}	$-\dfrac{\varphi}{4\pi}$	$O(1)$	$O(1)$

The new variance $\mathrm{Var}[\hat{\phi}_{\textbf{new}}]$ is $\ll \mathrm{Var}[\hat{\phi}]$ in the TDL ($\epsilon \ll \epsilon^{-1}$).

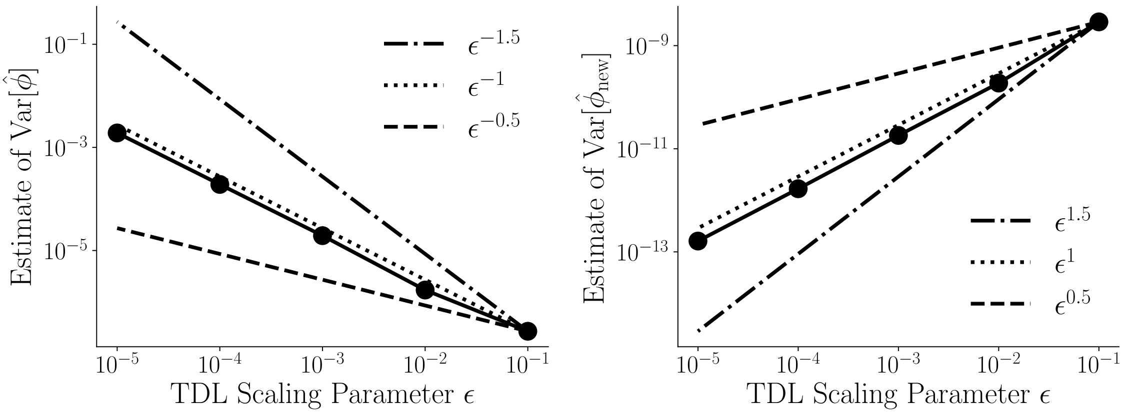

The new solution is incorrect on material interfaces.

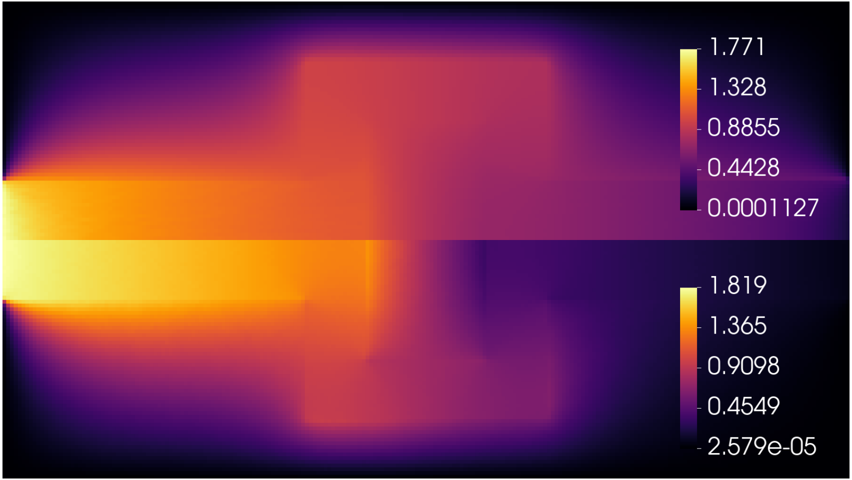

Modify the approach by replacing φ with $\bar{\varphi}$.

Before, we substituted $\psi = \frac{\varphi}{4\pi} + \tilde{\psi}$ to get:

$$\mathbf{\Omega} \cdot \nabla\tilde{\psi} + \sigma_t\tilde{\psi} = -\frac{1}{4\pi}(\sigma_a\varphi + \mathbf{\Omega} \cdot \nabla\varphi) + q\,, \tag{19a}$$

$$\tilde{\psi}(\mathbf{x}, \mathbf{\Omega}) = \psi_{\text{inc}}(\mathbf{x}, \mathbf{\Omega}) - \frac{\varphi(\mathbf{x})}{4\pi}\,, \quad \mathbf{x} \in \partial\mathcal{D} \text{ and } \mathbf{\Omega} \cdot \mathbf{n} < 0\,. \tag{19b}$$

Now, substitute $\psi = \frac{\bar{\varphi}}{4\pi} + \tilde{\psi}$ to get:

$$\mathbf{\Omega} \cdot \nabla\tilde{\psi} + \sigma_t\tilde{\psi} = \frac{\sigma_t}{4\pi}(\varphi - \bar{\varphi}) - \frac{1}{4\pi}(\sigma_a\varphi + \mathbf{\Omega} \cdot \nabla\bar{\varphi}) + q\,, \tag{20a}$$

$$\tilde{\psi}(\mathbf{x}, \mathbf{\Omega}) = \psi_{\text{inc}}(\mathbf{x}, \mathbf{\Omega}) - \frac{\bar{\varphi}(\mathbf{x})}{4\pi}\,, \quad \mathbf{x} \in \partial\mathcal{D} \text{ and } \mathbf{\Omega} \cdot \mathbf{n} < 0\,. \tag{20b}$$

Choose $\bar{\varphi}$ such that $\nabla\bar{\varphi}$ is well-defined and $\varphi - \bar{\varphi}$ is $O(1/\sigma_t)$.

	Fixed	Variable		
Volume	q	$\frac{\sigma_s}{4\pi}\varphi$	$O(\epsilon)$	$O(1/\epsilon)$
Boundary	ψ_{inc}	0	$O(1)$	N/A
Volume	q	$-\frac{1}{4\pi}(\sigma_a\varphi + \boldsymbol{\Omega}\cdot\nabla\varphi)$	$O(\epsilon)$	$O(1)$
Boundary	ψ_{inc}	$-\frac{\varphi}{4\pi}$	$O(1)$	$O(1)$
Volume	q	$\frac{\sigma_t}{4\pi}(\varphi - \bar{\varphi}) - \frac{1}{4\pi}(\sigma_a\varphi + \boldsymbol{\Omega}\cdot\nabla\bar{\varphi})$	$O(\epsilon)$	$O(?)$
Boundary	ψ_{inc}	$-\frac{\bar{\varphi}}{4\pi}$	$O(1)$	$O(1)$

Solve a transient heat conduction equation for $\bar{\varphi}$.

$$\frac{\partial \bar{\varphi}}{\partial t} = \nabla \cdot \frac{1}{\sigma_t} \nabla \bar{\varphi}, \quad \mathbf{x} \in \mathcal{D}\,, \tag{21a}$$

$$\bar{\varphi}(\mathbf{x}, 0) = \varphi(\mathbf{x}), \quad \mathbf{x} \in \mathcal{D}\,, \tag{21b}$$

$$\bar{\varphi}(\mathbf{x}, t) = \varphi(\mathbf{x}), \quad \mathbf{x} \in \partial\mathcal{D}\,. \tag{21c}$$

Take one small timestep such that,

$$\frac{\Delta t}{h^2} \frac{1}{\max_{\mathbf{x}} \sigma_t} \ll 1\,. \tag{22}$$

Discretize space using discontinuous finite elements.

Find $\bar{\varphi} \in Y_p$ such that,

$$\frac{\partial}{\partial t}\int u\,\bar{\varphi}\,\mathrm{d}x - \int_{\Gamma_b} u\left(\frac{1}{\sigma_t}\nabla\bar{\varphi}\right)\cdot\mathbf{n}\,\mathrm{d}s + \int \nabla u \cdot \frac{1}{\sigma_t}\nabla\bar{\varphi}\,\mathrm{d}\mathbf{x}$$
$$- \int_{\Gamma_0}\left\{\!\!\left\{\frac{1}{\sigma_t}\nabla\bar{\varphi}\cdot\mathbf{n}\right\}\!\!\right\}[\![u]\!]\,\mathrm{d}s + \sigma\int_{\Gamma_0}[\![\bar{\varphi}]\!]\left\{\!\!\left\{\frac{1}{\sigma_t}\nabla u\cdot\mathbf{n}\right\}\!\!\right\}\mathrm{d}s =$$
$$- \sigma\int_{\Gamma_b}\varphi\left(\frac{1}{\sigma_t}\nabla u\cdot\mathbf{n}\right)\mathrm{d}s - k\int_{\Gamma_b}\left\{\!\!\left\{\frac{1}{h}\frac{1}{\sigma_t}\right\}\!\!\right\}\varphi u\,\mathrm{d}s\,, \quad \forall u \in Y_p\,. \quad (23)$$

Discretize time using backward Euler.

Let Φ contain L^2 dofs for $\bar{\varphi}$. Then,

$$M \frac{\mathrm{d}\Phi}{\mathrm{d}t} = -K\Phi + f \,. \tag{24}$$

Backward Euler is,

$$M \frac{\Phi^{n+1} - \Phi^n}{\Delta t} = -K\Phi^{n+1} + f \,. \tag{25}$$

Thus,

$$(M + \Delta t K)\Phi^{n+1} = M\Phi^n + \Delta t\, f \,. \tag{26}$$

Define parameter α such that,

$$\Delta t = \alpha h^2 \left(\max_{\mathbf{x}} \sigma_t \right) \,. \tag{27}$$

The solution on material interfaces is no longer incorrect.

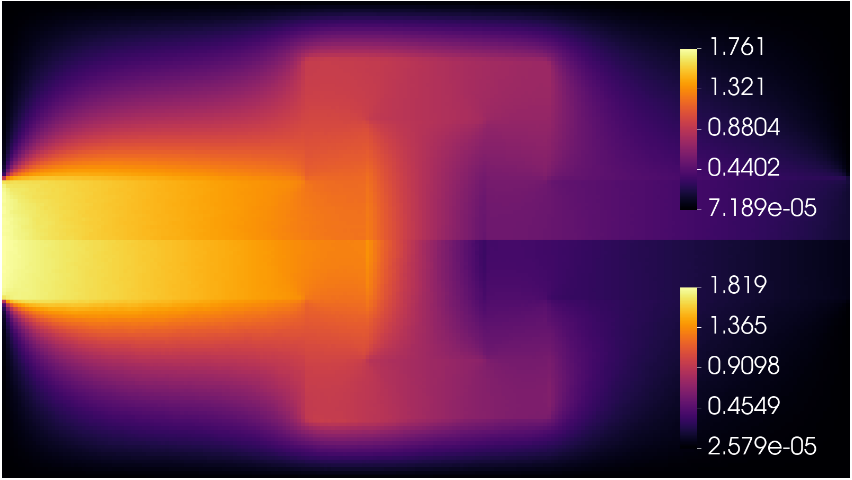

The generalized variance reduction fixes the noise issue.

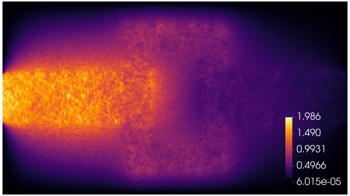

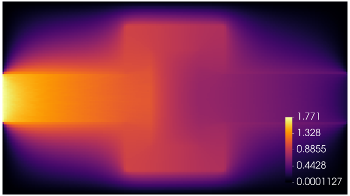

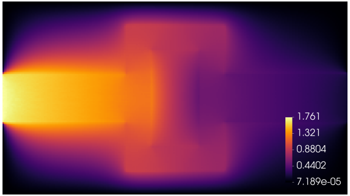

The figure of merit is much higher for HSM than for UMC.

	Runtime	Variance	FOM
HSM	0m 22s	$3.66 \cdot 10^{-4}$	124.2
UMC	41m 35s	$5.20 \cdot 10^{-5}$	7.7

Could HSM be competitive with IMD or DDMC?

	HSM	DDMC
Orders of magnitude speedups	✓	✓
No diffusion approximation	✓	×
No phase-space partitioning	✓	×
No issues with unstructured meshes	✓	×
No iteration	×	✓
No linear solver	×	✓
No difference formulation	×	✓
Demonstrated in production calculations	×	✓

Conclusion: the HSM method described in this talk seems useful.

~~Motivation~~

~~Prior Work~~

~~Hybrid Second Moment Method~~

- ~~Deterministic Component of HSM~~
- ~~Monte Carlo Component of HSM~~

~~Numerical Results~~

- ~~Method of Manufactured Solutions Verification~~
- ~~Noisy Crooked Pipe~~

~~Variance Reduction~~

- ~~Difference Formulation~~
- ~~Incorrect Crooked Pipe~~
- ~~Generalized Difference Formulation~~
- ~~Correct Crooked Pipe~~

Conclusion

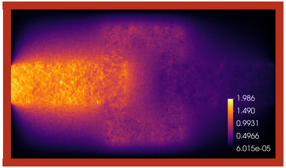

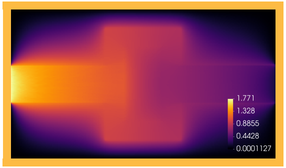

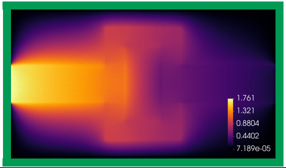

The future work for HSM is a path to production calculations.

1. time dependence, $\psi(\mathbf{x}, \mathbf{\Omega}, t)$
2. frequency dependence, $\psi(\mathbf{x}, \mathbf{\Omega}, t, \nu)$
3. 1D Spherical, 2D RZ, and 3D
4. hydrodynamics coupling
5. physical scattering
6. graphics processors
7. spectral line transport
8. high order

Progress Porting LLNL Monte Carlo Transport Codes to the AMD Instict MI300A APU at 1:25 PM today in Special Session on GPU Computing

llnl.gov/article/52336/llnl-dedicates-el-capitan-ushering-new-era-supercomputing-national-security

Only 8% of the HSM runtime is in the deterministic component.

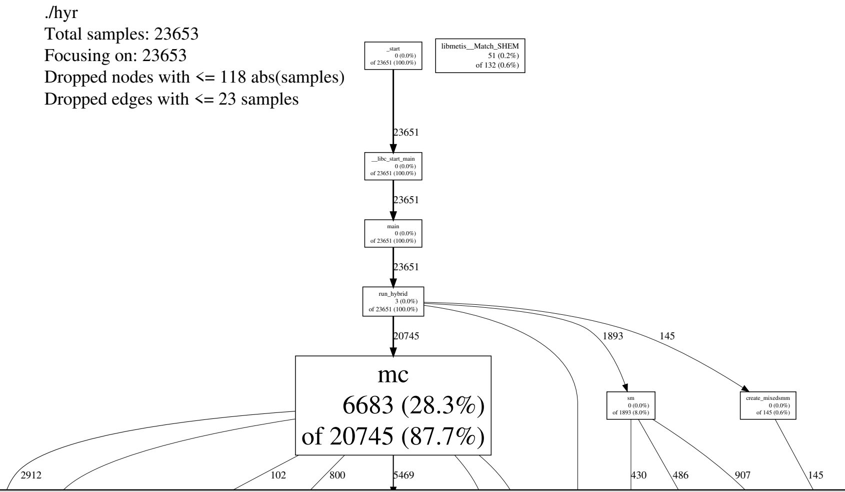

The HSM iteration converges quickly.

```
defaults="
runvars.convergence_criterion = 0.001;
runvars.num_bdr_src_particles = 16e6;
runvars.num_vol_src_particles = 16e6;
runvars.mesh = [[lcp5.mesh]];
runvars.output_root_filename = "

srun -n112 ./hyr lcp.lua -e "$defaults
[[hsm_lcp_16e6_16e6]]"
```

```
Running lcp5.mesh-16000000-16000000 (mesh-np)
The total weight is 0.50005
The total weight is -1.50598
Cycle 1: Maxres 0.00e+00 0.00e+00 Runtime 8.96e-01 4.78e+00
The total weight is -1.24976
Cycle 2: Maxres 4.41e-01 3.04e-01 Runtime 1.08e-01 2.49e+00
The total weight is -1.15745
Cycle 3: Maxres 2.13e-01 7.89e-02 Runtime 2.30e-01 8.06e-01
The total weight is -1.12240
Cycle 4: Maxres 9.70e-02 2.81e-02 Runtime 9.56e-02 8.10e-01
The total weight is -1.10688
Cycle 5: Maxres 3.88e-02 1.14e-02 Runtime 9.18e-02 8.07e-01
The total weight is -1.09918
Cycle 6: Maxres 1.71e-02 4.97e-03 Runtime 1.58e-01 8.26e-01
The total weight is -1.09509
Cycle 7: Maxres 8.47e-03 2.26e-03 Runtime 1.47e-01 8.03e-01
The total weight is -1.09284
Cycle 8: Maxres 4.21e-03 1.06e-03 Runtime 1.53e-01 8.16e-01
The total weight is -1.09158
Cycle 9: Maxres 2.11e-03 5.06e-04 Runtime 1.36e-01 8.08e-01
The total weight is -1.09085
Cycle 10: Maxres 1.06e-03 2.48e-04 Runtime 1.39e-01 8.06e-01
The total weight is -1.09044
Cycle 11: Maxres 5.31e-04 1.24e-04 Runtime 2.37e-01 8.11e-01
```

Resetting the PRNG seed makes the HSM iteration converge.

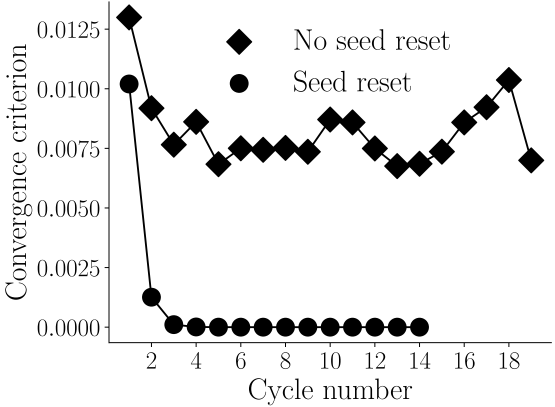

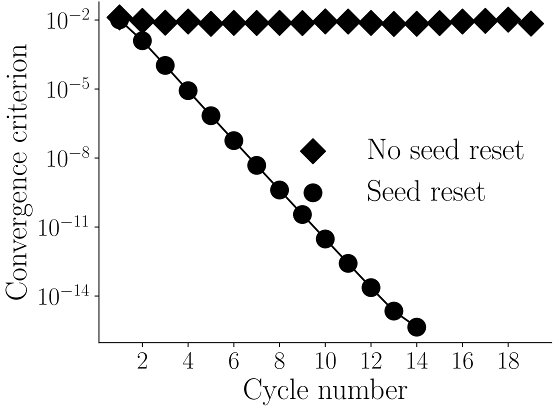

We sample volume sources uniformly.

$$\lim_{N\to\infty} \sum_{i=1}^{N} w_i = \int_{\mathcal{D}} \int_{\mathbb{S}^2} q \, \mathrm{d}\Omega \, \mathrm{d}\mathbf{x} \,, \tag{28a}$$

$$\int_{\mathcal{D}} \int_{\mathbb{S}^2} q \, \mathrm{d}\Omega \, \mathrm{d}\mathbf{x} \approx \frac{V}{N} \sum_{i=1}^{N} q(\mathbf{x}_i, \boldsymbol{\Omega}_i) \,, \tag{28b}$$

$$V = \int_{\mathcal{D}} \int_{\mathbb{S}^2} \mathrm{d}\Omega \, \mathrm{d}\mathbf{x} \,, \qquad \mathbf{x}_i = U(\mathcal{D}) \,, \qquad \boldsymbol{\Omega}_i = U(\mathbb{S}^2) \,. \tag{28c}$$

We sample boundary sources uniformly.

$$\lim_{M\to\infty} \sum_{i=1}^{M} w_i = \int_{\partial\mathcal{D}} \int_{\boldsymbol{\Omega}\cdot\mathbf{n}<0} |\boldsymbol{\Omega}\cdot\mathbf{n}|\psi_{\mathsf{inc}}\,\mathrm{d}\Omega\,\mathrm{d}\mathbf{x}\,, \tag{29a}$$

$$\int_{\partial\mathcal{D}} \int_{\boldsymbol{\Omega}\cdot\mathbf{n}<0} |\boldsymbol{\Omega}\cdot\mathbf{n}|\psi_{\mathsf{inc}}\,\mathrm{d}\Omega\,\mathrm{d}\mathbf{x} \approx \frac{S}{M}\sum_{i=1}^{M} |\boldsymbol{\Omega}_i\cdot\mathbf{n}|\psi_{\mathsf{inc}}(\mathbf{x}_i,\boldsymbol{\Omega}_i)\,, \tag{29b}$$

$$S = \int_{\partial\mathcal{D}} \int_{\boldsymbol{\Omega}\cdot\mathbf{n}<0} \mathrm{d}\Omega\,\mathrm{d}\mathbf{x}\,, \qquad \mathbf{x}_i = U(\partial\mathcal{D})\,, \qquad \boldsymbol{\Omega}_i = U(\mathbb{S}_h)\,. \tag{29c}$$

The iteration converges when the relative difference of successive iterates falls below a user-provided threshold, η.

$$\max_j \left(\frac{|\hat{\phi}_j^{(i-1)} - \hat{\phi}_j^{(i)}|}{\hat{\phi}_j^{(i-1)}} \right) < \eta \,, \qquad j = 1, \ldots, |\mathcal{T}| \,, \tag{30}$$

The error in the two scaling studies is computed differently

$$\text{Element scaling study error} = \frac{||\hat{\phi} - \bar{\phi}||_2}{|\mathcal{T}|}\,, \tag{31a}$$

$$\text{Particle scaling study error} = ||\hat{\phi} - \bar{\phi}||_2\,. \tag{31b}$$

Our code is only 5500 lines, not including dependencies.

Lines of code	Filename
20	wkt_conduction.h
22	wkt_mmsvars.h
26	system.c
37	eval.c
39	wkt_sources.h
57	wkt_runvars.h
481	write.c
746	hyr.c
1621	psmm.cpp
2463	mc.c
5512	total

Version	Library
1.14.3	hdf5
2.33.0	hypre
1.0.0	irep
5.4.6	lua
5.1.0	metis
4.6	mfem
4.40.3	parmetis
5.3.0	superlu

The UMC variance is highest in the optically-thick material.

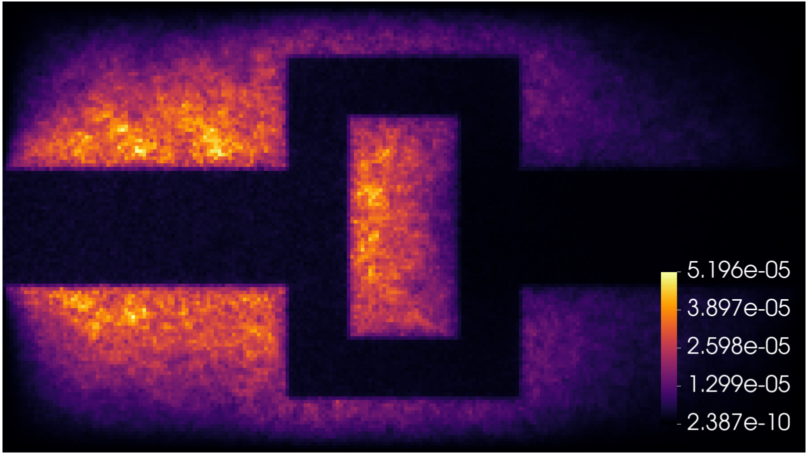

The HSM variance is highest at the inflow boundary.

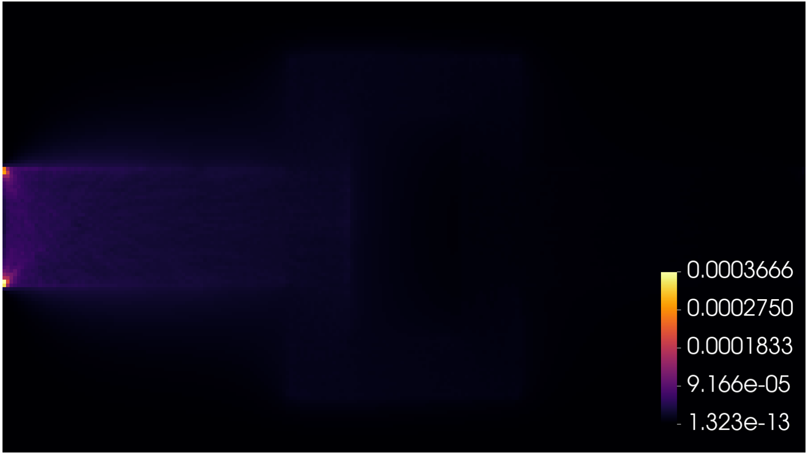

References I

[1] J. A. Fleck and J. D. Cummings. "An implicit Monte Carlo scheme for calculating time and frequency dependent nonlinear radiation transport." J Comput Phys, **volume 8**, pp. 313–342 (1971).

[2] M. L. Adams and E. W. Larsen. "Fast iterative methods for discrete-ordinates particle transport calculations." Progress in Nuclear Energy, **volume 40**(1), pp. 3–159 (2002).

[3] E. W. Larsen, J. E. Morel, and W. F. Miller Jr. "Asymptotic solutions of numerical transport problems in optically thick, diffusive regimes." J Comput Phys, **volume 69**(2), pp. 283–324 (1987). URL `https://www.sciencedirect.com/science/article/pii/0021999187901707`.

[4] A. B. Wollaber. "Four decades of implicit Monte Carlo." Journal of Computational and Theoretical Transport (2016).

[5] R. E. Alcouffe. "Diffusion Synthetic Acceleration Methods for the Diamond-Differenced Discrete-Ordinates Equations." Nuclear Science and Engineering, **volume 64**(2), pp. 344–355 (1977). URL `https://doi.org/10.13182/NSE77-1`.

[6] J. A. Fleck and E. H. Canfield. "A random walk procedure for improving the computational efficiency of the Implicit Monte Carlo method for nonlinear radiation transport." J Comput Phys, **volume 54**, pp. 508–523 (1984).

[7] N. Gentile. "Implicit Monte Carlo diffusion - An acceleration method for Monte Carlo time-dependent radiative transfer simulations." J Comput Phys, **volume 172**, pp. 543–571 (2001).

[8] J. D. Densmore, T. J. Urbatsch, T. M. Evans, and M. W. Buksas. "A hybrid transport-diffusion method for Monte Carlo radiative-transfer simulations." Journal of Computational Physics, **volume 222**(2), pp. 485–503 (2007). URL `https://www.sciencedirect.com/science/article/pii/S0021999106003639`.

References II

[9] V. Y. Gol'din. "A quasi-diffusion method of solving the kinetic equation." USSR Computational Mathematics and Mathematical Physics, **volume 4**, pp. 136–149 (1964).

[10] E. Lewis and W. Miller. "A comparison of p1 synthetic acceleration techniques." Transactions of the American Nuclear Society, **volume 23** (1976).

[11] M. A. Cooper and E. W. Larsen. "Automated Weight Windows for Global Monte Carlo Particle Transport Calculations." Nuclear Science and Engineering, **volume 137**, pp. 1–13 (2001).

[12] H. Park, D. A. Knoll, R. M. Rauenzahn, A. B. Wollaber, and J. D. Densmore. "A Consistent, Moment-Based, Multiscale Solution Approach for Thermal Radiative Transfer Problems." Transport Theory and Statistical Physics, **volume 41**(3-4), pp. 284–303 (2012). URL `https://doi.org/10.1080/00411450.2012.671224`.

[13] V. N. Novellino and D. Y. Anistratov. "Analysis of Hybrid MC/Deterministic Methods for Transport Problems Based on Low-Order Equations Discretized by Finite Volume Schemes." Transaction of American Nuclear Society, **volume 130** (2024).

[14] M. Pozulp, T. Haut, P. Brantley, and J. Vujic. "An Implicit Monte Carlo Acceleration Scheme." In Proceedings of the International Conference on Mathematics and Computational Methods Applied to Nuclear Science & Engineering (M&C 2023). Niagara Falls, Canada (2023).

[15] S. S. Olivier. High-Order Moment Methods for Thermal Radiative Transfer. Phd dissertation, University of California, Berkeley, Berkeley, CA (2022).

References III

[16] W. Pazner, T. Kolev, and P. S. Vassilevski. "Matrix-Free High-Performance Saddle-Point Solvers for High-Order Problems in $\boldsymbol{H}(\mathbf{div})$." SIAM Journal on Scientific Computing, **volume 46**(3), pp. B179–B204 (2024).

[17] S. Olivier, W. Pazner, T. S. Haut, and B. C. Yee. "A family of independent Variable Eddington Factor methods with efficient preconditioned iterative solvers." Journal of Computational Physics, **volume 473**, p. 111747 (2023). URL https://www.sciencedirect.com/science/article/pii/S0021999122008105.